Phonons in suspensions of hard sphere colloids: Volume fraction dependence

H. Kriegs
Max-Planck Institute for Polymer Research, P.O. Box 3148, 55128 Mainz, Germany

G. Petekidis
FO.R.T.H., Institute of Electronic Structure and Laser, P.O. Box 1527, 71110 Heraklion, Crete, Greece

G. Fytas
Max-Planck Institute for Polymer Research, P.O. Box 3148, 55128 Mainz, Germany and
FO.R.T.H., Institute of Electronic Structure and Laser, P.O. Box 1527, 71110 Heraklion, Crete, Greece

R. S. Penciu
FO.R.T.H., Institute of Electronic Structure and Laser, P.O. Box 1527, 71110 Heraklion, Crete, Greece

E. N. Economou
FO.R.T.H., Institute of Electronic Structure and Laser, P.O. Box 1527, 71110 Heraklion, Crete, Greece and Physics Department, University of Crete, P.O. Box 2208, 71003 Heraklion, Crete, Greece

A. B. Schofield
School of Physics, The University of Edinburgh, Mayfield Road, Edinburgh EH9 3JZ, United Kingdom

(Received 24 June 2004; accepted 3 August 2004)

The propagation of sound waves in suspensions of hard sphere colloids is studied as a function of their volume fraction up to random close packing using Brillouin light scattering. The rich experimental phonon spectra of up to five phonon modes are successfully described by theoretical calculations based on the multiple scattering method. Two main types of phonon modes are revealed: Type *A* modes are acoustic excitations which set up deformations in both the solid (particles) and the liquid (solvent) phases; for type *B* modes the stress and strain are predominantly localized near the interface between the solid particles and the surrounding liquid (interface waves). While the former become harder (increase their effective sound velocity) as the particle volume fraction increases the latter become softer (the corresponding sound velocity decreases). © *2004 American Institute of Physics.* [DOI: 10.1063/1.1798973]

I. INTRODUCTION

Wave propagation in microstructured materials is of both fundamental and practical importance due to the rich physics involved and the potential technological applications in the field of nanomaterials and sensors. More specifically the study of propagation of electromagnetic waves in composite random or periodic media led to the development of the field of photonic band gap materials[1–3] while that of elastic waves involving a higher number of material parameters (densities and sound velocities)[4–11] revealed specific composite structures, called phononic crystals, which exhibit spectral gaps. Colloidal suspensions are natural candidates as model microstructured materials due to the size of their structural units, namely, colloidal particles of submicron size and due to the fact that they form crystalline phases with lattice constants of the order of 1 to few particle diameters. Moreover, crystal structures of such dimensions (of the order of the wavelength of light) may ideally be studied by inelastic light scattering probing the propagation of acoustic waves in the GHz frequency range. Given the richness of the colloidal chemistry, and the variety of systems with numerous applications, the exploitation of the dispersion relations in model hard sphere colloidal suspensions in the liquid, crystalline, and glassy phase is of both fundamental and practical importance.

The first Brillouin scattering studies of hard sphere colloidal suspensions revealed only two propagating longitudinal modes utilizing a five-pass Fabry-Perot interferometer.[12] However, more recently, the use of a six-pass tandem Fabry-Perot interferometer allowed us to detect a much richer Brillouin spectrum in several microstructured systems such as liquid suspensions of soft micellar particles,[13] block copolymer lamellar forming system,[14] and suspensions of hard sphere colloids in the fluid, crystalline, and glass phase.[15,16] A variety of acoustic and opticlike modes were detected and attributed to the interplay of the acoustic phonon in the solvent matrix with the single particle vibrational eigenmodes. In a previous paper[16] we have presented experimental results together with theoretical predictions for the rich phonon spectra of colloidal systems of low and high elastic contrast. Here we extend this study providing experimental data along with theoretical calculations which describe the evolution of the phonon modes as the particle volume fraction ϕ is systematically increased from the fluid to the crystalline and glassy state. The experimental phonon spectra at several scattering wave vectors q were compared with theoretical calculations of (i) the dispersion relation of the frequency ω_n vs the wave number k for various phonon branches ($n=1,2,\ldots$), (ii) the light scattering intensity, (iii) the elastic field distribution, and (iv) the single scattering resonance frequencies.

The rest of the paper is organized as follows: In Sec. II, we briefly describe the experimental technique and the colloidal systems. In Sec. III we present the experimental inelastic light scattering spectra and the volume fraction dependence of the phonon dispersion relation $\omega_n(q)$, compare the experimental with the theoretical dispersion relations, and discuss the physical origin of the phonon modes and their volume fraction dependence. Finally, the conclusions are presented in Sec. IV.

II. EXPERIMENT

A. Fabry-Perot interferometry

Polarized Rayleigh-Brillouin spectra arising from thermal density fluctuations in the system were recorded at different scattering angles by a six-pass tandem Fabry-Perot interferometer (FPI).[16] A solid state Nd-YAG laser ($\lambda = 532$ nm) operating at 150 mW output power, together with the incident beam optics (a beam splitter for the reference beam, a focusing lens, and a Glan-Thomson polarizer) were mounted on the arm of a goniometer to allow a variation of the scattering wave vector $q=(4\pi n/\lambda)\sin(\theta/2)$ (n is the refractive index of the medium) over one order of magnitude. The scattered light with selected polarization determined by the analyzer was detected by an avalanche photon diode connected with the multichannel analyzer. Each spectrum $I(q,\omega)$ was recorded at two free spectral ranges (7.5 GHz and 30 GHz) in order to achieve both high resolution and broad frequency range. Typical accumulation time for each spectrum was about 30 min. The stabilization of the FPI was maintained over days using the reference beam during the scanning of the frequency ± 0.6 GHz about the central Rayleigh line by means of a synchronized shutter. Hence, the strong elastic ($\omega=0$) scattered light from the samples does not enter the FPI.

B. Samples

Colloidal suspensions were prepared at various volume fractions in the liquid, crystalline, and glass region.[17] The particles were poly-methylmethacrylate (PMMA) spheres sterically stabilized by chemically grafted chains of poly-12-hydroxystearic acid chains (typical thickness of 10 nm) in an almost refractive index matching solvent (mixture of 70% *cis*-decalin with 30% tetralin). They have a diameter $d = 364$ nm and a size polydispersity $\sigma=0.06$; both were determined by static and dynamic light scattering in dilute suspensions.

Samples in the liquid, crystalline, and glass state were prepared by successive dilutions of a random closed packed (RCP) sample obtained by centrifugation and the volume fraction was determined in the coexistence region ($0.494 < \phi < 0.545$). The present system comprising of PMMA particles suspended in the *cis*-decalin and tetralin mixture is characterized by a relatively low elastic constant contrast between the particles and the solvent. The longitudinal velocity inside the PMMA particles is $c_l = 2800$ m/s and the transversal is $c_t = 1400$ m/s while in the the solvent we have $c_l = 1500$ m/s. The densities of the particle and solvent are 1180 kg/m^3 and 926 kg/m^3, respectively.

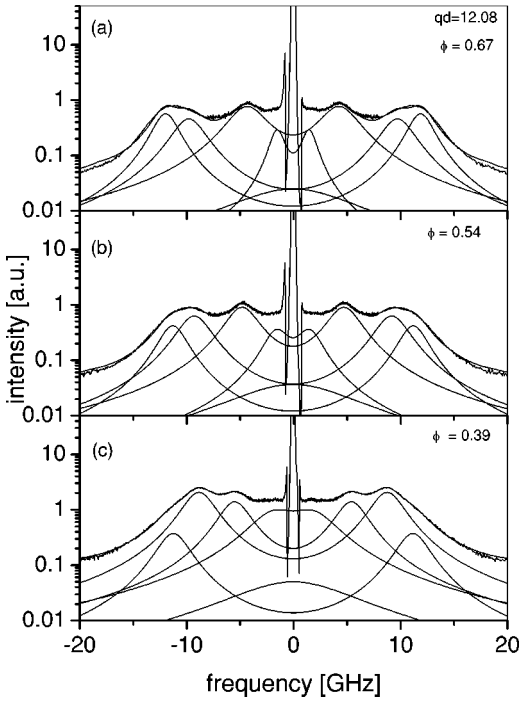

FIG. 1. Brillouin spectra of a colloidal suspension of PMMA spheres in decalin/tetralin with colloid volume fraction (a) $\phi=0.67$ (RCP glass), (b) $\phi=0.54$ (crystalline state), and (c) $\phi=0.39$ (liquid state), at high scattering wave vector $q=0.033$ nm^{-1} ($qd=12.08$). The experimental Brillouin spectrum are expressed as a sum of several Lorentzians (solid lines) convoluted with the instrumental function. Note the increase of the highest frequency mode contribution with increasing particle volume fraction.

III. RESULTS AND DISCUSSION

Figures 1 and 2 show high resolution polarized (VV) Brillouin spectra from colloidal suspensions in the liquid ($\phi=0.39$), crystalline ($\phi=0.54$), and glass (RCP, $\phi = 0.67$) state at high and low qd values, respectively. The frequency region, which lies approximately ± 0.5 GHz from the central peak is provided by the reference beam used for the stabilization of the tandem Fabry-Perot interferometer. The spectra may be fitted by a sum of Lorentzian lines plus an anisotropic broad background convoluted by the instrumental function; the broad central line arises from the anisotropic (depolarized) scattering of the solvent. A rich spectrum (up to five Brillouin doublets in Figs. 1 and 2) is observed at all the three different states of the colloidal dispersion independently of the volume fraction. However, the relative intensities do change as the volume fraction increases and some of these modes are better seen in an ordered state rather than in an amorphous one. Note that the polarized spectra are distinctly different from the featureless depolarized (VH) spectra which are mainly due to the optically anisotropic solvent.

The location of the Lorentzians defines the experimental phonon frequencies ω_n at each wave vector q. In Fig. 3 we show the experimental dispersion of the resolved acoustic excitations $\omega_{\mathbf{q},n}$ for two volume fractions in the liquid and glassy state as a function of qd. The experimental linear dispersion of the longitudinal phonon in the solvent (crosses) is also shown. As discussed in detail in our previous paper,[16] three main groups of phonon modes are revealed in Fig. 3.

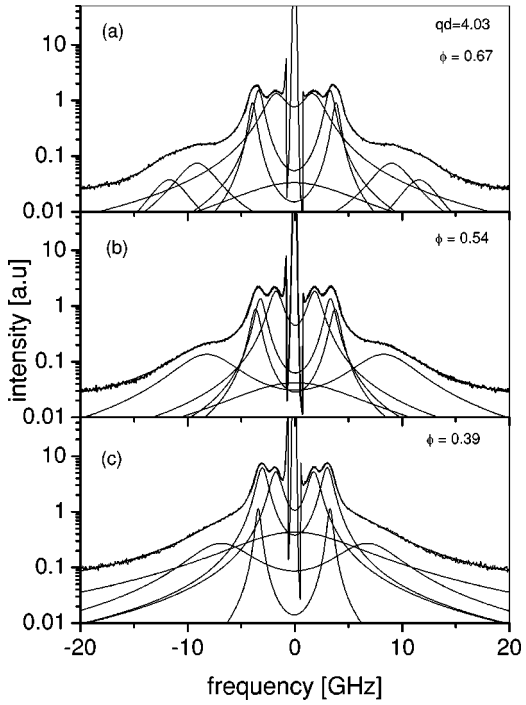

FIG. 2. Brillouin spectra from suspension with colloid volume fraction (a) $\phi=0.67$ (RCP glass), (b) $\phi=0.54$ (crystalline state), and (c) $\phi=0.39$ (liquid state), at low $q=0.011\ \mathrm{nm}^{-1}$ ($qd=4.03$). Note the increase of the contribution of the mode with $f\simeq 4$ GHz with ϕ.

(i) The high frequency modes at low q's, with an optic-like q-independent frequency, correspond approximately to eigenmodes of individual spheres.

(ii) The phonon modes with frequency higher than the corresponding frequency of the pure solvent are acoustic-like ($\omega\sim q$) (type A modes).

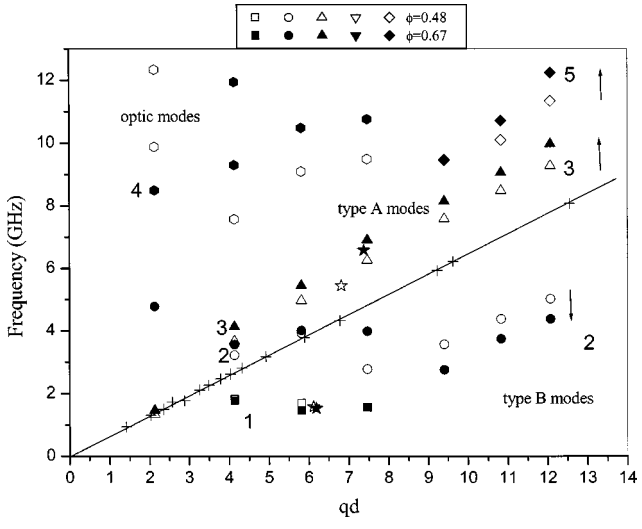

FIG. 3. Phonon dispersion relations. The solid line fits the measured linear dispersion for the longitudinal phonon in the solvent (+). All symbols represent experimental points in the frequency-wave vector plane: Open symbols ($\phi=0.48$), solid symbols ($\phi=0.67$). The various modes are enumerated as indicated: mode 1 (squares), mode 2 (circles), mode 3 (up triangles), mode 4 (hexagons), and mode 5 (diamonds). The asterisks represent theoretical results; the corresponding elastic field distribution is shown in Figs. 7 and 8.

(iii) The low frequency phonon modes with frequencies lower than that of the pure solvent are either q independent at low q's (inside the first Brillouin zone) or, at high q's, acoustic-like with an effective sound velocity smaller than that in the solvent (type B modes).

The experimental spectra were compared with theoretical band structure calculations for infinite fcc lattices which have been presented in detail in our previous paper.[16] Briefly, we used the complex multiple scattering method, which is able to describe the case of composites made up of solid scatterers embedded in a fluid host. The multiple scattering formalism is based on an expansion in spherical harmonics, Y_{lm}. The resulting series is truncated ($l\leqslant l_{\max}$) without appreciable error as long as ω is less than a value, $\omega(l_{\max})$, which increases with $l_{\max}$. The only disadvantage of this method is that the computational time increases very quickly with $l_{\max}$. This is the reason for which we limit our band structure calculations at 7 GHz. Since some of the samples are in an amorphous (glassy or liquid) state, we calculated the band structure for few different $\vec{k}$ orientations.

To compare with experimental data we kept only the modes which are strongly coupled to the incident photon giving a strong light scattering intensity ($I/I_{\max}>0.1$, where $I_{\max}$ is the maximum value of the calculated intensity). Furthermore, for high q, we extended the multiple scattering band structure calculations to higher Brillouin zones (up to the seventh) extending the maximum wave vector to $qd=8$. The agreement between theory and experiment is reasonable. However, a detailed comparison is not easy because: (i) Experimental data from amorphous or polycrystalline samples are compared with calculations assuming perfect fcc order and (ii) the inelastic light scattering intensity is a very sensitive function of the structure, scattering wave vector, and scattering frequency. Consequently, a phonon by phonon comparison is not feasible.

The nature of the two type of phonon modes were elucidated by theoretical calculations of the elastic field distribution.[16] At low frequencies and q's ($qd\simeq 2$) type A modes are propagating acoustic modes confined predominantly in the solvent with sound velocity essentially equal to that of the pure solvent mixture. However, at high q's the morphological details of the composite medium are revealed in the sound propagation as a splitting of the modes due to an interaction between the acoustic phonons with individual particle eigenmodes. In this way at high qd values hybrid propagating modes are produced corresponding to phonons that propagate both in the liquid and the solid phase. Although such modes were observed before,[12] the detection of such a rich phonon spectrum was made possible only with the use of high resolution tandem Fabry-Perot interferometry.[13,16] As the volume fraction increases, type A modes shift towards higher frequencies as expected for sound waves propagating in a composite medium with a higher average solid content. Type B modes, at low frequencies, represent an alternative channel of wave propagation in the composite material in which the excitation is mainly localized around the interface between the solid and the liquid. As the volume fraction is increased the frequency of these modes decrease in contrast to the trend followed for type A

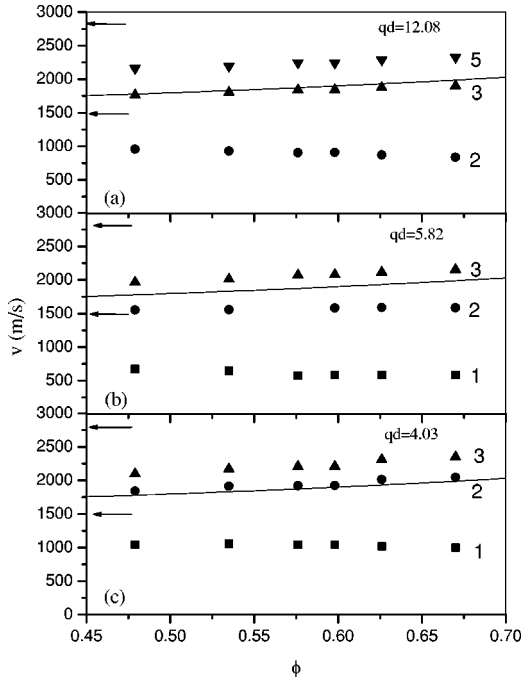

FIG. 4. Volume fraction dependence of the sound velocity $v(=\omega/q)$ corresponding to the main modes, as indicated, at three different wave vectors: (a) $qd=12.08$, (b) $qd=5.82$, and (c) $qd=4.03$. The arrows point out the velocity of sound in the solid and liquid phase. The solid line corresponds to the calculation of the velocity using the effective-medium model.

modes. The volume fraction dependence of the type *A* and type *B* modes are in agreement with the behavior of the two modes observed by Ye and co-workers.[12]

In Fig. 4 we show the volume fraction dependence of the sound velocity $v(=\omega/q)$ calculated at three different q's for the three stronger type *A* and type *B* modes. The arrows indicate the velocity of sound in the solid (PMMA) and liquid phase (mixed solvent) while the solid line represents the corresponding velocity in a composite medium with an average elastic modulus β according to $1/\beta=\phi/\beta_s+(1-\phi)/\beta_l$ (effective medium model)[18,19] where β_s and β_l are the elastic moduli of the solid PMMA particle and the liquid, respectively. Type *A* modes exhibit high sound velocity which increases with volume fraction at low and high q's. On the other hand, type *B* modes, with sound velocity lower than that of the pure solvent, become softer (lower sound velocity) at high q's as the volume fraction is increasing while at low q's are almost unaffected.

However, there are modes which exhibit a type *A* behavior at low q's but behave like type *B* modes at high q's. Such a behavior is shown in Fig. 3 where the modes with frequencies higher than that of the solvent at low q's (around 3 GHz) become harder as ϕ increases whereas the modes with similar frequencies at high q become softer. None of these propagate with the exact velocity calculated for an effective medium at all q's, suggesting that even type *A* modes are complicated propagating hybrid modes. Although such excitations propagate in both phases, the system cannot be represented by an average effective solid medium. A further confirmation for such a description is the existence of more than one type *A* modes at high q's resulting from a splitting

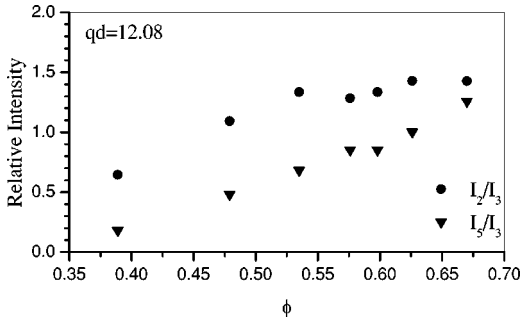

FIG. 5. Volume fraction dependence of the ratio of the intensities of the two main modes (2 and 5) to that of the acoustic mode 3 at $qd=12.08$ as indicated.

of the main mode at intermediate q's (see Fig. 3). We should note that our measurements were restricted to $qd>2$; hence there might as well be a regime at low qd values were the average medium description holds quantitatively.

In Fig. 5 we show the intensities, at high qd, of the two main phonon modes (I_2 and I_5) relative to that of the acoustic mode (I_3) as a function of the volume fraction. The second type *A* mode, resulting from a splitting at high q's of the main acoustic type *A* mode, is observed only at high volume fractions (above $\phi=0.39$) and gains intensity as volume fraction increases. Mode 2 (of type *B*) is also gaining intensity relative to the main mode 3 as ϕ increases exhibiting, however, a finite intensity at the low ϕ's.

Figure 6 shows the q dependence of the attenuation coefficient,[20] Γ/q^2, for the two main phonon modes as determined from the Lorentzian fits of the phonon spectra (see Figs. 1 and 2) at the highest volume fraction. For $qd>4$, the type *A* mode 3 exhibits the expected, for a propagating acoustic phonon, q^2 hydrodynamic line-width dependence, whereas Γ/q^2 of the nonacoustic type *B* mode 2 displays a residual q dependence. The deviation at the lowest qd measured reflects the splitting of the acoustic mode observed at $qd\simeq 4$. Based on the short phonon life time $(1/\Gamma)$ of the highest q in the PMMA suspensions, the acoustic excitations decays within distance of few particle diameters. This is

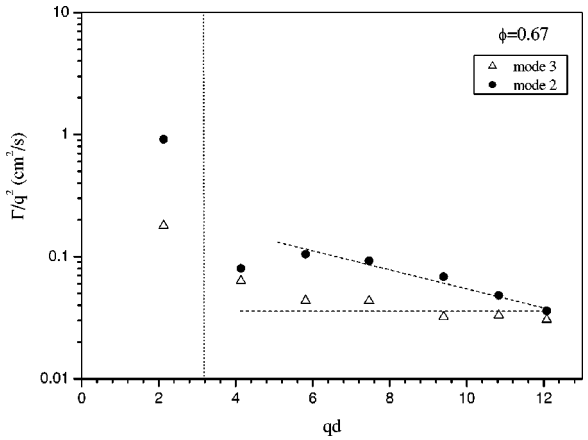

FIG. 6. Scattering wave vector dependence of the line width in the form of Γ/q^2, for mode 2 (●) and mode 3 (△) at $\phi=0.67$. The lines are to guide the eye. The perpendicular dotted line indicates the qd value above which a splitting of the main acoustic mode is observed.

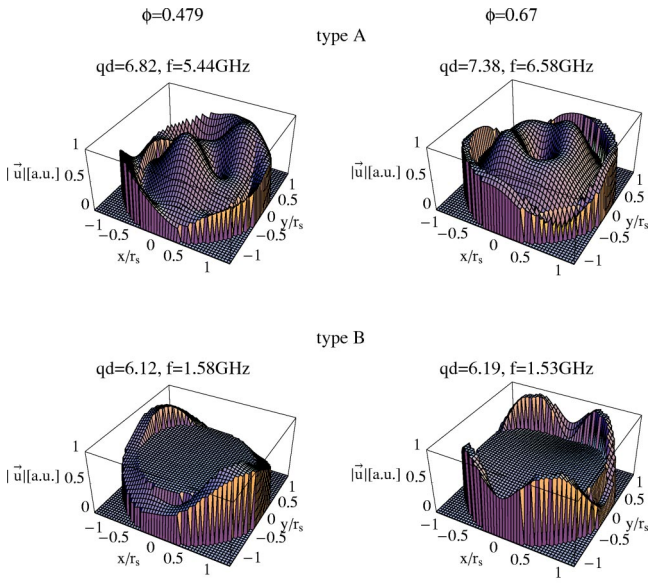

FIG. 7. Two-dimensional plots of the displacement vector, $|\mathbf{u}(\mathbf{r})|$ as $\mathbf{r}$ moves in the x, y plane perpendicular to $\mathbf{k}$ for two different frequency modes at low (0.479) and high (0.67) volume fractions. The top two plots represent type A modes of phonon excitations and the two bottom ones type B modes with qd and f values as indicated. This modes are indicated (with an asterisk) in the dispersion plot of Fig. 3.

probably the reason that glassy and crystalline phases of PMMA suspensions display similar phonon dispersions.[16]

The elastic field distribution calculated at different volume fractions provides a visualization of the phonon excitations and can help to elucidate their volume fraction dependence. Figure 7 shows a two-dimensional plot of the displacement vector, $|\mathbf{u}(x,y,z)|$, corresponding to the Brillouin modes with the strongest scattering intensities predicted theoretically by the complex multiple scattering method in the vicinity of the experimental Brillouin modes (Fig. 3) at two different volume fractions. The Wigner-Seitz cell was approximated by a coated sphere made up of a solid PMMA core and a shell of liquid solvent. The volume of the coated sphere is equal with that of the Wigner-Seitz cell.

For the higher frequency, type A modes, the field is concentrated mostly inside the PMMA spheres (Fig. 7) giving rise to considerable deformations and stresses. This finding is consistent with a high frequency mode and it confirms that such modes propagate in the medium through both phases. Hence, at higher particle volume fractions where the PMMA contribution is larger, the sound velocity increases, and the frequency of the mode is higher at a given q as found experimentally. Such volume fraction dependence is generic for all type A modes (mode 3, 5, as well as mode 2 at low qd). We notice that all Brillouin modes with frequency larger than that of the solvent propagate with velocities which increase as the volume fraction of the solid phase increases in agreement with the notion of excitations propagating through a harder average medium. In the same context, the intensity of the assorted Brillouin line increases with volume fraction (Fig. 5).

In contrast to type A modes, the low frequency and high q type B modes (Fig. 7), propagate predominantly near the interface between the particles and the solvent. Such modes may propagate inside the medium by hopping from one particle to another, a process that is obviously favored as the volume fraction increases. Moreover, the finite constant value of the displacement vector inside the particle suggests that type B modes involve motions of the solid particle as an almost rigid body inside the liquid medium. As a result the strain-stress within the particles is minimum and the eigenfrequency is low. With increasing volume fraction higher harmonics of the surface waves are excited as revealed by the two bottom plots of Fig. 7. Such generic behavior may be caused by the proximity of neighboring spheres which increases at high volume fractions rendering collisions of the caged particle with its neighbors more probable. These surface modes essentially correspond to the flow of the solvent next to the particle surface as it is squeezed out of the region between particles. To further elucidate the character of the type B modes, we plot the x component of the displacement vector u_x. Figure 8 shows such a plot for the highest volume fraction, $\phi=0.67$, at large values of qd. For the type A mode ($f=6.58$ GHz), u_x clearly shows a phonon mode that sets up strains (and hence stresses) both inside the solid particle and in the surrounding liquid, whereas the low frequency phonon mode (type B mode, $f=1.55$ GHz) represents an almost rigid motion of the particle in the suspension which creates interfacial waves. This interpretation was further supported by calculating $|\nabla\times\mathbf{u}|/|\mathbf{u}|$ and $|\nabla\cdot\mathbf{u}|/|\mathbf{u}|$ for the two modes. The strain measuring quantities were almost ten times larger for mode A than for mode B inside the spherical particles; furthermore, for the type B modes both $|\nabla\times\mathbf{u}|/|\mathbf{u}|$ and $|\nabla\cdot\mathbf{u}|/|\mathbf{u}|$ were concentrated near the interface between the particle and the surrounding liquid. Finally the increase of the intensity I_2, assorted with this type B mode, with volume fraction (Fig. 5) supports its interfacial character and in the same context the shorter life time (Fig. 6) of this mode as compared to type A modes is not unexpected.

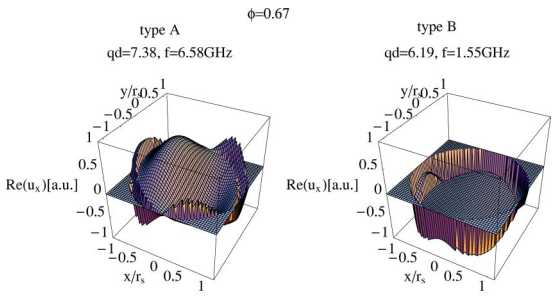

FIG. 8. The projection of the displacement vector along the x axis for the two phonon modes at $\phi=0.67$ shown in Fig. 7. The left one corresponds to a type A mode and the right one to type B mode.

IV. CONCLUSIONS

Employing high resolution Brillouin light scattering we have measured the phonon modes in colloidal suspensions as a function of the particle volume fraction. We detected up to five phonon modes in liquid, crystal, and glassy suspensions of hard sphere colloids up to the volume fraction of random

close packing. The experimental phonon frequencies were successfully described by theoretical calculations of the dispersion relation of the frequencies ω_n vs the wave number k and the elastic field distribution based on the multiple scattering method. Based on this agreement, the two main types of phonon modes are related with acoustic excitations which propagate through both particles and solvent (type A modes) and modes which are mainly localized at the interface between the colloids and the solvent (type B modes). The sound velocity associated with type A modes increases with particle volume fraction whereas that of the type B modes decreases.

ACKNOWLEDGMENTS

We thank Dr. M. Kafesaki for providing computational codes. G.P. acknowledges funding by a Marie Curie Fellowship of the European Community program under Contract No. ERBFMBICT983380. Partial financial support of the Grant No. GPAN-2013555 is gratefully acknowledged. Financial support by EU Grant Nos. FMRX-CT96-0042 and HPRN-CT-2000-00017 are also acknowledged.

[1] C. M. Soukoulis, *Photonic Crystals and Light Localization in 21st Century* (Kluwer Academic Publishers, Dordrecht, 2001).
[2] J. D. Joannopoulos, R. D. Meade, and J. N. Winn, *Photonic Crystals: Molding the Flow of Light* (Princeton University Press, Princeton, 1995).
[3] K. Sakoda, *Optical Properties of Photonic Crystals*, Springer Series in Optical Sciences, Vol. 80 (Springer, Berlin, 2001).
[4] M. M. Sigalas and E. N. Economou, J. Sound Vib. **158**, 377 (1992).
[5] M. S. Kushwaha and P. Halevi, Appl. Phys. Lett. **69**, 31 (1996).
[6] M. Kafesaki and E. N. Economou, Phys. Rev. B **60**, 11993 (1999).
[7] D. Garcia-Pablos, M. M. Sigalas, F. R. Montero de Espinosa, M. Torres, M. Kafesaki, and N. Garcia, Phys. Rev. Lett. **84**, 4349 (2000).
[8] Z. Liu, X. Zhang, Y. Mao, Y. Y. Zhu, Z. Yang, C. T. Chan, and P. Sheng, Science **289**, 1734 (2000).
[9] M. Kafesaki, R. S. Penciu, and E. N. Economou, Phys. Rev. Lett. **84**, 6050 (2000).
[10] I. E. Psarobas, N. Stefanou, and A. Modinos, Phys. Rev. B **62**, 278 (2000).
[11] S. Yang, J. H. Page, Z. Liu, M. L. Cowan, C. T. Chan, and P. Sheng, Phys. Rev. Lett. **88**, 104301 (2002).
[12] J. Liu, L. Ye, D. A. Weitz, and P. Sheng, Phys. Rev. Lett. **65**, 2602 (1990); L. Ye, J. Liu, P. Sheng, and D. A. Weitz, Phys. Rev. E **48**, 2805 (1993).
[13] R. S. Penciu, G. Fytas, E. N. Economou, W. Steffen, and S. N. Yannopoulos, Phys. Rev. Lett. **85**, 4622 (2000).
[14] A. M. Urbas, E. L. Thomas, H. Kriegs, G. Fytas, R. S. Penciu, and E. N. Economou, Phys. Rev. Lett. **90**, 108302 (2003); G. Tommaseo, R. S. Penciu, G. Fytas, E. N. Economou, T. Hashimoto, and N. Hadjichristidis, Macromolecules **37**, 5006 (2004).
[15] R. S. Penciu, M. Kafesaki, G. Fytas, E. N. Economou, W. Steffen, A. Hollingsworth, and W. B. Russel, Europhys. Lett. **58**, 699 (2002).
[16] R. S. Penciu, H. Kriegs, G. Petekidis, G. Fytas, and E. N. Economou, J. Chem. Phys. **118**, 5224 (2003).
[17] P. N. Pusey, in *Liquids, Freezing and the Glass Transition*, edited by J. P. Hansen, D. Levesque, and J. Zinn-Justin (Elsevier, Amsterdam, 1991).
[18] P. Sheng, in *Homogenization nd Effective Moduli of Materials and Media*, edited by J. L. Ericksen, D. Kinderlehrer, R. Kohn, and J.-L. Lions (Springer, New York, 1986) p. 196.
[19] Z. Hashin, J. Appl. Math. Mech. **29**, 143 (1962).
[20] B. J. Berne and R. Pecora, *Dynamic Light Scattering with Applications to Chemistry, Biology and Physics*, (Dover, New York, 2000), p. 256.